Quasienergy spectrum of complex atoms

E. Meşe
Department of Physics, University of Dicle, Diyarbakır, Turkey

R. M. Potvliege
Department of Physics, Durham University, Durham DH1 3LE, United Kingdom

(Received 17 July 2007; published 14 February 2008)

Representative sections of the quasienergy spectrum of argon and of alkali-metal atoms are presented for wavelengths between 250 nm and 800 nm and excursion amplitudes up to $\alpha_0=20$ a.u. The variation of the quasienergy spectrum with the wavelength of the laser field is discussed. It is shown that large-scale changes in its topology arise from laser-induced degeneracies with states without physical high-intensity or low-intensity limits.

DOI: 10.1103/PhysRevA.77.023414 PACS number(s): 32.80.Rm, 42.50.Hz

I. INTRODUCTION

The dynamics of an atom exposed to a long laser pulse can be understood from the properties of its dressed states and from the interplay between these dressed states at multiphoton resonances [1–5]. These states are eigenstates of the Hamiltonian describing the atom in the presence of a laser field of constant intensity and constant frequency. They are described by state vectors of the Floquet form, namely, for a monochromatic field of angular frequency ω, state vectors of the form

$$|\Psi(t)\rangle = e^{-i\epsilon t/\hbar}\sum_{N=-\infty}^{\infty} e^{-iN\omega t}|\mathcal{F}_N\rangle, \tag{1}$$

where the harmonic components $|\mathcal{F}_N\rangle$ are time independent. The quasienergy, ϵ, is complex for the dressed bound states this work is concerned with: Denoting by $\epsilon^{(0)}$ the zero-field limit of ϵ, by Δ the ac Stark shift of the state, and by Γ its ionization width,

$$\epsilon = \epsilon^{(0)} + \Delta - i\Gamma/2. \tag{2}$$

Both Δ and Γ vary with the intensity of the field and with its frequency. When allowed by the selection rules, multiphoton resonances occur at those intensities and frequencies where two dressed states have quasienergies with real parts differing by an integer multiple of $\hbar\omega$ [6]. Such resonances are often referred to as Freeman resonances. They frequently occur in strong laser pulses, due to the large Stark shift bound states may incur at high intensity, and are a major source of low energy photoelectrons in the multiphoton ionization of atoms [7]. There is strong evidence that they are also major contributors to the high energy plateau part of the above-threshold ionization (ATI) spectrum for pulses of sufficiently long durations [8–13]. Although quasienergy energy spectra of atoms in a laser field have been compiled for more than 20 years, much of the past effort has been concentrated on hydrogen and/or on wavelengths in the uv or xuv [14]. It is only recently that a comprehensive quasienergy map of a complex atom has been calculated for a longer laser wavelength, namely, argon at 800 nm [13]. Some of the low lying excited states were found to shift in an intricate and apparently random way, making the spectrum more complex at that wavelength than at high frequencies. How the spectrum evolves as the wavelength increases was subsequently explored by calculations at 400 and 600 nm wavelength [15]. We much extend these previous calculations, compare argon to several alkali-metal atoms, and describe, in detail, the wavelength dependence of a representative part of the quasienergy spectrum.

It is well known that when the photon energy much exceeds the binding energy of the ground state, the quasienergy spectrum is simple: in the high frequency limit, the quasienergies of the dressed atom become identical to the energies of the bound states supported by an effective time-independent potential, the "dressed potential" [3,16–19]. This potential (and therefore, in a first approximation, the quasienergies of the real atom) depends on the intensity and on the frequency through a single parameter, the excursion amplitude α_0 of an electron freely oscillating in the field. [Assuming the laser to be linearly polarized and described by the electric field $F(t)=F_0\cos(\omega t)$, $\alpha_0=F_0/\omega^2$ in atomic units.] In contrast, the quasienergy of a state whose binding energy is close to or less than the photon energy may completely depart from the corresponding energy level of the dressed potential, which complicates the spectrum at long wavelengths. In particular, the deeply bound states may shift considerably relative to the highly excited states and perturb the latter through multiphoton resonances. However, even in this case, the energy levels of the dressed potential that have a binding energy much smaller than the photon energy can be expected to have a counterpart in the quasienergy spectrum of the real atom. If the intensity increases to high values and the single active electron approximation still holds, one can also expect that the quasienergy spectrum tends to converge toward the same high-frequency spectrum as atomic hydrogen, since at high intensities the active electron has a large probability to be far from the core and thus interacts with it mainly through the long-range Coulomb potential. This convergence was demonstrated for argon in Ref. [15].

The low-intensity quasienergy spectrum tends to vary more with wavelength than the high-intensity spectrum. Consequently, a same high-intensity dressed state may have different zero-field limits at different wavelengths. The interchanges between resonant dressed states as the intensity var-

ies have been analyzed long ago [20,21]: The real parts of the two quasienergies may describe a direct crossing or an avoided crossing, depending on the relative magnitude of their imaginary parts, and the crossing may be direct at some wavelengths and avoided at others. The corresponding adiabatic quasienergy curves swap limits when the crossing changes between direct and avoided. Such changes normally happen at complex values of the electric field amplitude at which the two quasienergies are degenerate [22]. However, for some states a degeneracy may occur at a real electric field amplitude, at a certain wavelength, which gives rise to a "laser-induced degeneracy" [23–25]. As is shown by our results, the way in which the high-intensity quasienergy spectrum connects to the weak-field spectrum changes with wavelength through a series of laser-induced degeneracies. We find that a number of degeneracies leading to a large scale rearrangement of the spectrum involve dressed states that acquire unphysical properties at high intensity and/or at low intensity.

Previous studies of the multiphoton ionization of argon at 800 nm wavelength have established that ATI spectra in excellent agreement with experiment can be obtained within the single-active electron approximation, up to intensities of about 100 TW cm^{-2} and possibly beyond (i.e., up to values of α_0 of at least 16 Bohr radii at that wavelength) [11]. In these calculations, the interaction between the active electron and the core is represented by a simple potential which is chosen in such a way that its field-free bound states energies match those of the real atom. The fact that this model accurately reproduces the experimental positions of the Freeman resonances indicates that it also yields faithful quasienergy spectra. We have adopted it in the present work. We also show quasienergy spectra of lithium, sodium, potassium, and rubidium obtained by using similar model potentials [26], and compare these atoms to atomic hydrogen.

The method followed for calculating the quasienergy spectrum is outlined in Sec. II. The results are presented in Sec. III, and conclusions are drawn in Sec. IV. Atomic units (a.u.) are used throughout the paper, except where otherwise indicated.

II. METHOD

For argon, we represent the atom by a single-active electron moving in the field of the potential [11]

$$W(r) = -\frac{1}{r}[1 + 5.25e^{-0.97r} + 11.75e^{-3.7131r}], \tag{3}$$

where r is the distance of the electron to the nucleus. Apart for the deeply bound $1s$, $2s$, $2p$, and $3s$ states supported by this potential, which have no counterpart in the spectrum of the real atom, and the $4s$ state, for which there is a 2% difference, the corresponding field-free energy levels coincide within 0.02 eV or less with the centroids of the experimental fine-structure multiplets of the series converging to the $3p^5\ ^2P^o_{3/2}$ threshold. For lithium, sodium, potassium, and rubidium, the model potentials are those proposed by Klapisch [26] and have the form

TABLE I. Parameters of the Klapisch potentials for the alkali-metal atoms considered in this work, in a.u. [26].

	A	B	α	β
Li	2	10.31	7.9	3.898
Na	10	23.513	7.902	2.688
K	18	10.596	3.474	1.725
Rb	36	6.429	3.333	1.369

$$W(r) = -\frac{1}{r}[1 + Ae^{-\alpha r} + Bre^{-\beta r}]. \tag{4}$$

The parameters A, B, α, and β were obtained by Klapisch by fitting the energy levels of the model to those of the experimental values. They are given in Table I.

Clearly, $W(r) = -1/r$ in the calculations for atomic hydrogen.

We follow the same approach for obtaining the quasienergy spectra as in Refs. [13,15]. The numerical techniques used in the calculation are described in Ref. [27]. Briefly, the time-dependent Schrödinger equation for the model atom in a monochromatic laser field is reduced to a system of coupled time-independent equations for the harmonic components $|\mathcal{F}_N\rangle$, the "Floquet equations." This system is solved in position space subject to Siegert boundary conditions. To this end, the harmonic components are expanded on a basis of spherical harmonics and of complex radial Sturmian functions. The quasienergies are then found as generalized eigenvalues of a complex matrix representing the Hamiltonian of the system, which is done by Arnoldi iterations. Spurious solutions arising from numerical inaccuracies and solutions representing approximate dressed continuum states rather than the relevant dressed bound states are eliminated by ignoring the quasienergies that are not stable with respect to changes of the basis set.

We work within the dipole approximation, neglect spin-orbit coupling, and assume the polarization to be linear and parallel to the direction of quantization of the angular momenta. The dressed bound states $|\Psi(t)\rangle$ are therefore eigenvectors of the projection of the orbital angular momentum operator on the polarization axis; the corresponding eigenvalues are $m\hbar$, $m = 0, \pm 1, \pm 2, \ldots$. (The quasienergies do not depend on the sign of m.) Moreover, the solutions of the Floquet equations decouple into two parity classes, according to whether, under a reflection about the origin, $|\mathcal{F}_N\rangle \rightarrow (-1)^N|\mathcal{F}_N\rangle$ or $|\mathcal{F}_N\rangle \rightarrow -(-1)^N|\mathcal{F}_N\rangle$ for all values of N. We distinguish the corresponding quasienergies by the quantum number σ such that $\sigma = 1$ when $|\mathcal{F}_N\rangle \rightarrow (-1)^N|\mathcal{F}_N\rangle$ and $\sigma = -1$ when $|\mathcal{F}_N\rangle \rightarrow -(-1)^N|\mathcal{F}_N\rangle$. Since Eq. (1) determines ϵ only within an integer multiple of the photon energy, a same dressed state $|\Psi(t)\rangle$ is associated with infinitely many quasienergies $\epsilon + n\hbar\omega$, $n = 0, \pm 1, \pm 2, \ldots$. The corresponding solutions of the Floquet equations belong to the same parity class when n is even and to opposite parity classes when n is odd. The complete bound state quasienergy spectrum is therefore composed of a double infinity of interlacing Brillouin zones, each zone spanning a range of values of Re ϵ of

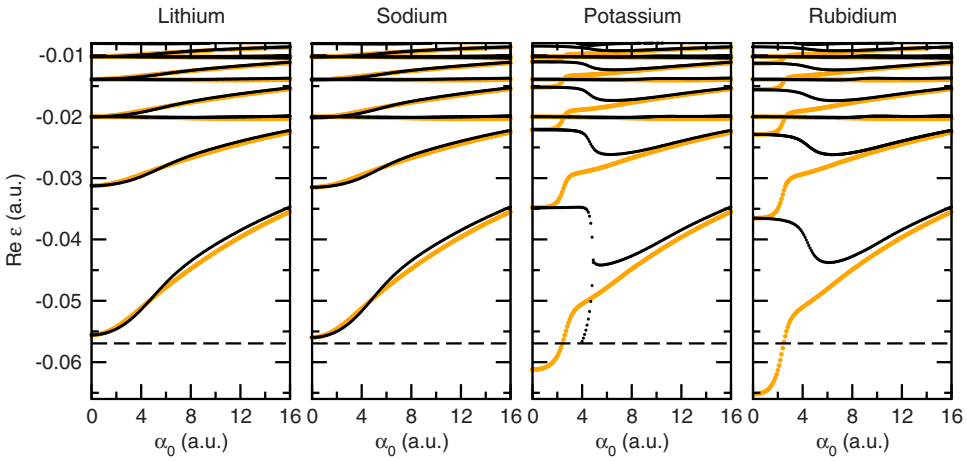

FIG. 1. (Color online) ($\sigma=1, |m|=2$) quasienergy spectrum of lithium, sodium, potassium, and rubidium, at the wavelengths of 250 nm (orange dots) and 800 nm (black dots). A dashed line is drawn at Re $\epsilon=-\hbar\omega$ at 800 nm; no results are given for Re $\epsilon<-\hbar\omega$.

extension $\hbar\omega$ and repeating itself with period $2\hbar\omega$. The spectra shown in Sec. III are representative regions of one Brillouin zone for either $m=0$ or $m=\pm 2$.

All calculations are done in the velocity gauge, with the term quadratic in the vector potential removed from the Hamiltonian by a gauge transformation. Hence the real part of the quasienergies of the dressed highly excited states remains almost constant when the intensity increases, while the real part of the quasienergies of the states whose zero-field binding energy much exceeds the photon energy shifts downward by approximately $-U_p$, where U_p is the ponderomotive energy.

III. RESULTS AND DISCUSSION

A. High frequency regime

We start by examining how the quasienergy spectrum of the $|m|=2$ dressed states of lithium, sodium, potassium, and rubidium changes between 250 nm and 800 nm wavelength. A large region of a $\sigma=1$ Brillouin zone is shown for each atom in Fig. 1. For each quasienergy belonging to this region, Re ϵ is plotted as a function of the excursion amplitude α_0. (Recall that α_0 is proportional to the square root of the intensity and inversely proportional to the square of the frequency; as noted in the Introduction, α_0 is the natural intensity parameter in the high frequency regime.) Each calculated point is shown as a dot; the mesh in α_0 is fine enough that in most cases the data points form continuous curves. The dashed lines indicate the lower limit of the Brillouin zone, where Re $\epsilon=-\hbar\omega$, at 800 nm. An infinity of dressed Rydberg states, not represented in the diagrams, accumulate immediately below these dashed lines. From bottom to top, the dressed states visible in the lithium spectrum converge for $\alpha_0\to 0$ to the $3d$, $4d$, $5d$, and $5g$, $6d$ and $6g$, and $7d$, $7g$, and $7i$ $m=\pm 2$ states of the field-free atom. The dressed g and i states shift very little at the intensities considered and come out as straight horizontal lines in the diagrams.

At 250 nm, the photon energy much exceeds the binding energy of all the field free $m=2$ states for all four species. This wavelength is thus representative of the high frequency regime. There is no significant difference between lithium and sodium (and between these two atoms and hydrogen), nor for $\alpha_0>3$ a.u. between these species and potassium and rubidium. The dressed d states of the latter two move to lower values of Re ϵ in the zero-field limit, owing to their larger quantum defect. When plotted versus α_0, as done in Fig. 1, the 800 nm spectrum remains close to the 250 nm spectrum, for all intensities in the cases of lithium and sodium and for $\alpha_0\gg 4$ a.u. in the cases of potassium and rubidium. The agreement is that expected in the high frequency regime. In contrast to the lighter alkali metals, however, at low values of α_0 the quasienergies of the dressed d states of potassium and rubidium do not follow the same trajectories at 800 nm than at 250 nm.

For instance, consider the dressed $5d$ state of potassium, for which Re $\epsilon=-0.022$ a.u. in the absence of field ($\alpha_0=0$). At 250 nm, this state follows essentially the same trajectory

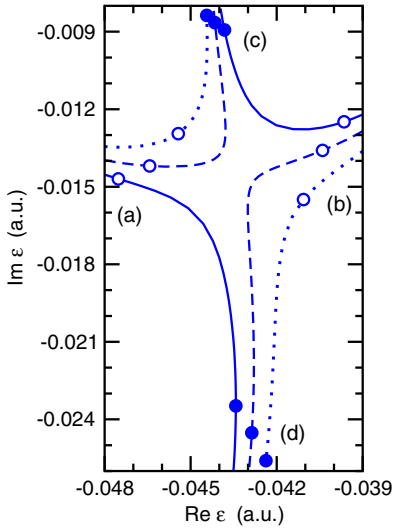

FIG. 2. (Color online) Trajectories described by the quasienergies of two dressed states of potassium at a laser wavelength of 800 nm (solid curves), 790 nm (dashed curves), or 780 nm (dotted curves). Open circles: $\alpha_0=4.8$ a.u.; closed circles: $\alpha_0=5$ a.u. The quasienergy curves converge toward the following limits outside of the range covered by the diagram. (a) Low-α_0 trajectory of the dressed $3d$ state at high frequency. (b) Low-α_0 trajectory of the dressed $4d$ state at high frequency. (c) High-α_0 trajectory of the dressed $3d$ state at high frequency. (d) High-α_0 trajectory of the unphysical state.

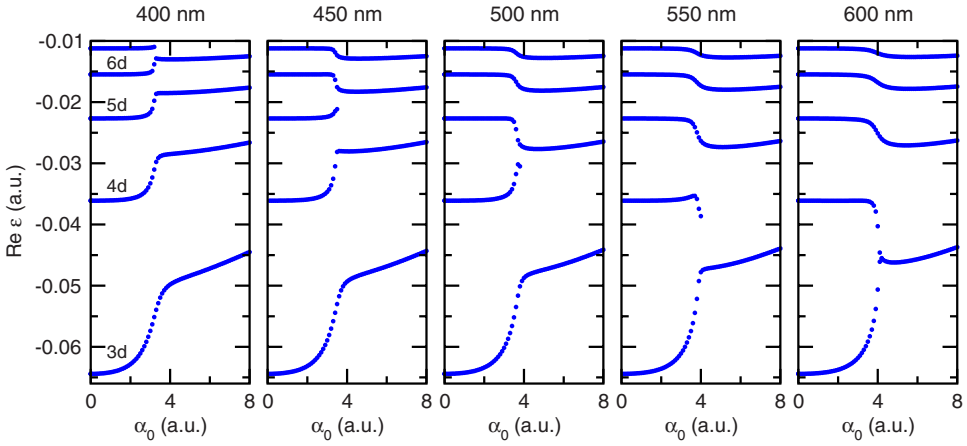

FIG. 3. (Color online) ($\sigma=1,|m|=2$) quasienergy spectrum of argon from 400 nm to 600 nm wavelength. For clarity, only the dressed $3d$, $4d$, $5d$, $6d$, and $7d$ $m=\pm 2$ states have been represented.

as the $5d$ states of lithium and sodium apart from a minor difference in position for $\alpha_0<3$ a.u. It starts at −0.022 a.u. rather than −0.020 a.u. and hardly shifts at first, before moving rapidly *upward* at $\alpha_0\approx 2$ a.u. By contrast, at 800 nm, this state shifts little at first, up to $\alpha_0\approx 4$ a.u., at which point it moves rapidly *downward* until following a trajectory similar to that the dressed $4d$ state has at 250 nm. Similarly, at 800 nm and for high α_0 the dressed $4d$ state follows a trajectory similar to that the $3d$ state has at shorter wavelengths. The dressed $3d$ state, which starts at −0.061 a.u. in zero field, cannot be followed much beyond $\alpha_0=5$ a.u. at 800 nm as its ionization width becomes rapidly too large for this state to be amenable to a calculation on the basis sets used in this work. The restructuration of the spectrum between 250 nm and 800 nm is the same for rubidium as for potassium. It affects the whole of the d series.

The interaction between the dressed $3d$ and $4d$ states of potassium is analyzed in Fig. 2. This diagram shows how the quasienergies move in the complex plane for three different wavelengths close to 800 nm and for values of α_0 close to 5 a.u. As α_0 approaches 5 a.u. from below, the dressed $3d$ state moves toward increasing values of $\mathrm{Re}\,\epsilon$, and the dressed $4d$ state moves in the opposite direction. They both enter in the region spanned by the diagram a little below $\alpha_0=4.8$ a.u., respectively from the left and from the right. At 800 nm, the dressed $4d$ state then describes an upward trajectory, with a rapid decrease of $|\mathrm{Im}\,\epsilon|$, as this state starts following the high-frequency $3d$ dressed state. At the same wavelength, the $3d$ state moves along a downward trajectory for $\alpha_0\gtrsim 5$ a.u., and its imaginary part becomes more and more negative. The ionization width of this state keeps increasing at higher values of α_0, until it becomes so large that we cannot follow its quasienergy further due to numerical instabilities. We note that an imaginary part of −0.03 a.u. corresponds to an ionization lifetime of only 167 a.u., which is not much longer than to the duration of an optical cycle at 800 nm (110 a.u.). This state thus loses all physical significance for $\alpha_0\gg 5$ a.u. At 790 nm and shorter wavelengths, it is the low-intensity $4d$ state, not the low-intensity $3d$, which connects to the high-intensity unphysical state. The change in the low-intensity limit of the $3d$ high-intensity quasienergy curve thus takes places through a laser-induced degeneracy occurring at a wavelength a little below 800 nm.

We have found curve interchanges similar to those affecting the $m=2$ spectra of potassium and rubidium in the quasienergy spectrum of argon, both for $m=2$ and $m=3$. How they develop for that atom as the wavelength increases is shown in Fig. 3. At 450 nm, the $3d$ and $4d$ states have similar trajectories as at 400 nm and both states can be followed continuously from $\alpha_0=0$ to $\alpha_0=8$ a.u. (and beyond). However, between 400 and 450 nm interchanges occur in the $6d$ and $5d$ curves. At 450 nm, the latter cannot be followed much beyond $\alpha_0=4$ a.u. Between 450 and 500 nm, the dressed $5d$ state reconnects to the high-α_0 part of the $4d$ trajectory, the $4d$ state becoming unphysical for $\alpha_0\gg 4$ a.u. The low-α_0 $4d$ curve starts shifting downwards at longer wavelengths, until it reconnects to the high-α_0 part of the $3d$ trajectory a little below 600 nm. At this point, this is now the low-α_0 part of the $3d$ trajectory which connects to the unphysical state. The restructurization of the spectrum thus develops over a range of wavelengths. It proceeds through a succession of laser-induced degeneracies at which a state which has no well defined high-intensity limit swaps the low-intensity dressed state it connects to.

The range of wavelengths and excursion amplitudes at which this restructurization occurs depends on the details of the short range part of the model potential. We have not observed it in lithium and sodium, and it does not seem to be present in atomic hydrogen.

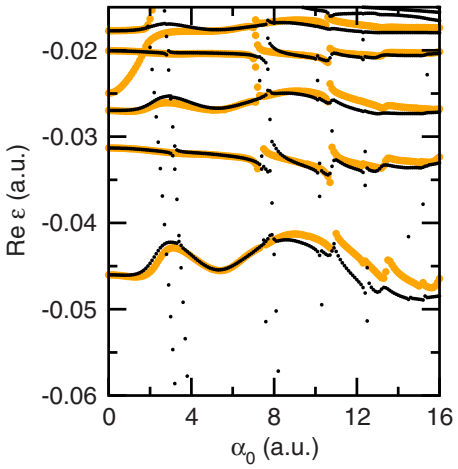

FIG. 4. (Color online) ($\sigma=-1,m=0$) quasienergy spectrum of argon at the wavelengths of 300 nm (black dots) and 350 nm (orange dots). The dressed ground state and the dressed $3s$ state are represented at 300 nm.

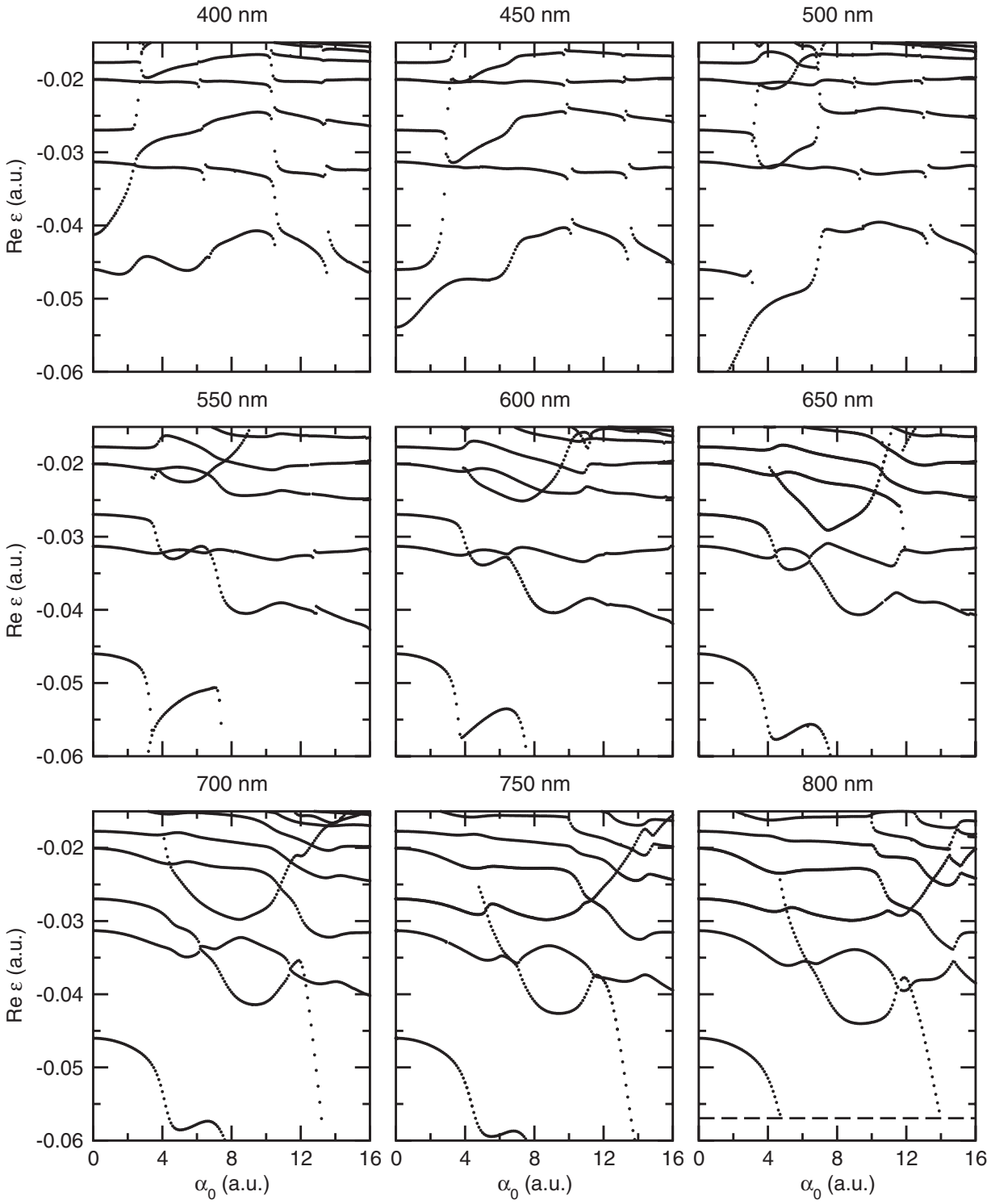

FIG. 5. ($\sigma=-1, m=0$) quasienergy spectrum of argon between 400 and 800 nm. The dressed ground state and the dressed $1s$, $2s$, $2p$, and $3s$ states supported by the model potential are not represented. A dashed line is drawn at Re $\epsilon=-\hbar\omega$ at 800 nm; no results are given for Re $\epsilon<-\hbar\omega$.

B. Interaction with low-lying states

We now turn to the interaction between low-lying states and dressed excited states. As noted above, quasienergies come in infinite combs of eigenvalues with identical imaginary parts and real parts differing by an integral multiple of the photon energy. Hence, if $\epsilon^{(0)}$ denotes the zero-field quasienergy of a dressed bound state, $\epsilon^{(0)}=-I_p+n^{(0)}\hbar\omega$, where I_p is the binding energy of the state in the field-free spectrum and $n^{(0)}$ is an integer. When the photon energy is smaller than the binding energy of the lowest bound state, Brillouin zones necessarily include quasienergies with differ-

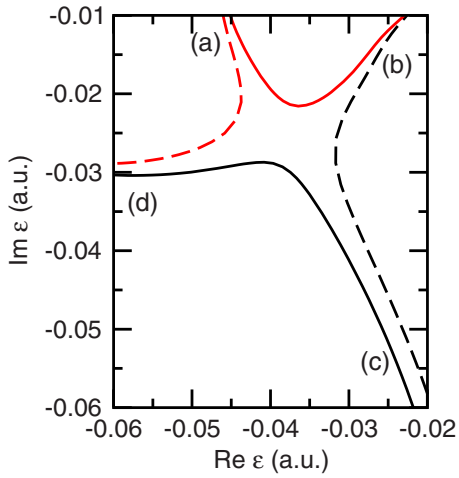

FIG. 6. (Color online) Trajectories described by the quasienergies of two dressed states of argon at a laser wavelength of 480 nm (solid curves) or 490 nm (dashed curves), for $\alpha_0 \approx 3$ a.u. The quasienergy curves converge toward the following limits outside of the range covered by the diagram. (a) Low-α_0 trajectory of the dressed $5p_{m=0}$ state. (b) High-α_0 trajectory of the dressed $7p_{m=0}$ state. (c) Low-α_0 trajectory of the light-induced state. (d) High-α_0 trajectory of the light-induced state.

ent values of $n^{(0)}$. The relative zero-field positions of two quasienergies of different $n^{(0)}$ values vary with ω, which makes the low-intensity part of the quasienergy spectrum wavelength dependent.

As a first example, part of the $(\sigma=-1, m=0)$ spectrum of argon is shown in Fig. 4 for two short wavelengths, 300 and 350 nm. All the dressed states contributing to this Brillouin zone are indicated, except the dressed $1s$, $2s$, and $2p$ states supported by the model potential. (These states have no counterpart in the spectrum of the real atom and their binding energy is too low for them to interact with the dressed excited states of interest.) From bottom to top, the quasienergy curves starting at $\alpha_0=0$ in the 300 nm spectrum belong to the dressed $5p$, $4f$, $6p$, $5f$, and $7p$ $m=0$ states, all with $n^{(0)}=0$. The same five states are also present and start from the same zero-field positions at 350 nm; the additional curve starting at Re $\epsilon=-0.025$ a.u. pertains to the dressed $4s$ state (with $n^{(0)}=1$). In the 300 nm spectrum, the data points aligned along oblique lines belong either to the dressed ground state or to the spurious dressed $3s$ state supported by the potential. Both have a binding energy much larger than the photon energy at that wavelength; as a result, they shift (almost) like $-U_p$. For clarity, these two states are not shown in the 350 nm spectrum.

The dressed excited states shift little on the whole, except at the intensities where they undergo avoided crossings with the ground state or, in some cases, with the dressed $3s$ state. These crossings occur at different intensities and at different wavelengths. A more significant difference between the two wavelengths is that at 350 nm, the dressed $7p$ state is disrupted at $\alpha_0 \approx 2$ a.u. by an avoided crossing with the dressed $4s$ state: While at 300 nm the high-α_0 part of the $7p$ quasienergy curve connects to the field-free $7p$ state in the zero-field limit, if one ignores a few minor avoided crossings with the dressed ground state, at 350 nm it connects to the field-free $4s$ state.

How the low-intensity part of the $(\sigma=-1, m=0)$ spectrum of argon evolves as the wavelength increases from 400 to 800 nm is shown in Fig. 5. The spectrum passes through a number of changes between these two wavelengths, the details of which can be found by comparing the diagrams. Of particular interest are the rearrangement of the spectrum accompanying the intrusion of the dressed $4s$ state and the large scale changes involving laser-induced degeneracies with states with unphysical features in the low- and/or the high-intensity limit.

At wavelengths above 350 nm, the zero-field position of the dressed $4s$ state $(n^{(0)}=1)$ shifts to increasingly negative values of Re ϵ: The corresponding quasienergy curve starts at -0.041 a.u. at 400 nm, at -0.054 a.u. at 450 nm, and at -0.064 a.u. at 500 nm. This motion is accompanied by a succession of changes in the high-α_0 limit of this curve. While at 350 nm it connects to the high-α_0 $7p$ curve, at 400 nm it connects to the high-α_0 $6p$ curve, and at 450 and 500 nm to the high-α_0 $5p$ curve. Simultaneously, the low-α_0 $5p$ and $6p$ curves acquire different high-intensity limits: At 400 nm, the field-free $6p$ state connects to a quasienergy curve much higher in the spectrum; at 450 nm, the field-free $5p$ state connects to the high-α_0 $7p$ curve; while at 500 nm it connects to a state without physical high-intensity limit. At that wavelength, the low-α_0 $5p$ curve and the high-α_0 $7p$ curve cannot be followed, respectively, much beyond and much below $\alpha_0 \approx 3$ a.u.

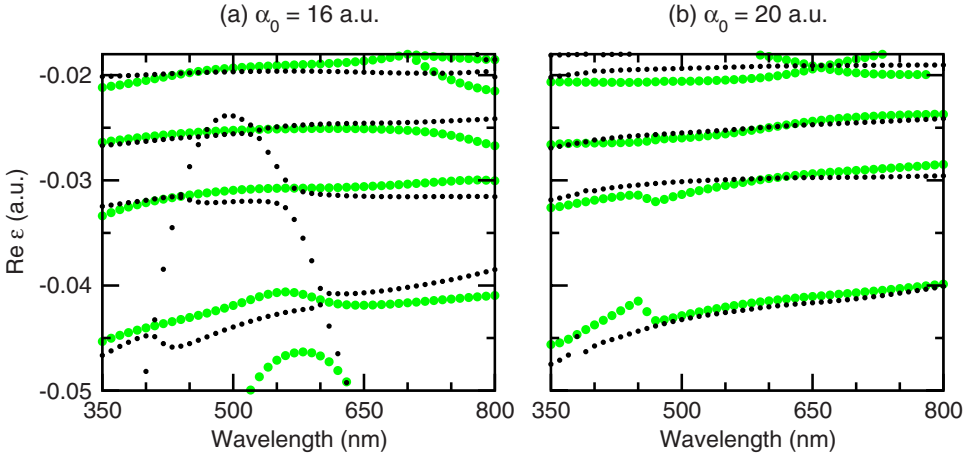

FIG. 7. (Color online) $(\sigma=-1, m=0)$ quasienergy spectrum of argon (black dots) and of atomic hydrogen (green dots) at wavelengths between 350 and 800 nm. (a) $\alpha_0=16$ a.u. (b) $\alpha_0=20$ a.u.

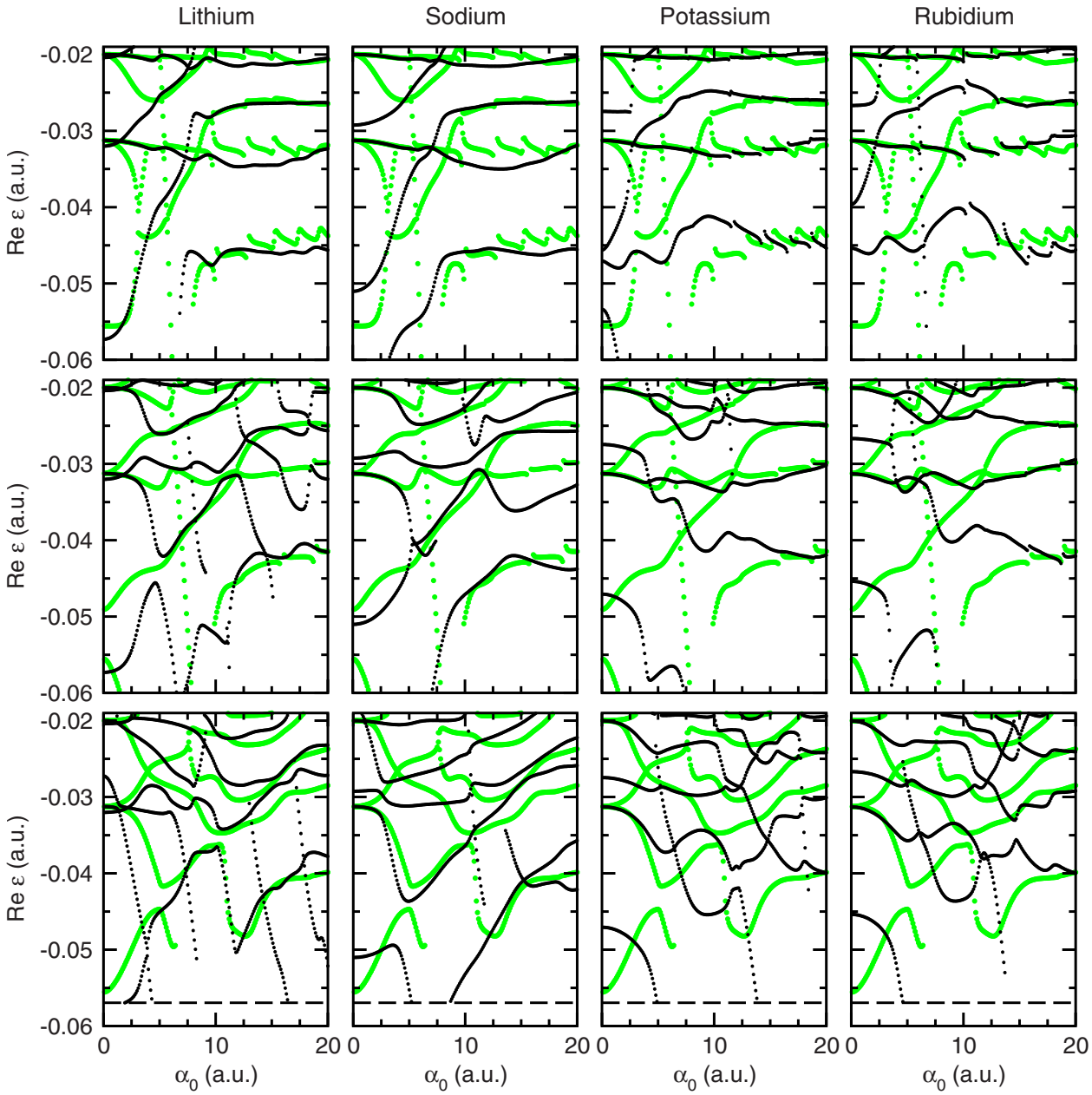

FIG. 8. (Color online) ($\sigma=-1, m=0$) quasienergy spectrum of lithium, sodium, potassium, and rubidium (black dots) and of atomic hydrogen (green dots) at a wavelength of 400 nm (top row), 600 nm (middle row), and 800 nm (bottom row). Dashed lines are drawn at Re $\epsilon=-\hbar\omega$ in the 800 nm spectra; no results are given for Re $\epsilon<-\hbar\omega$. Dressed low lying states have been removed by representing only the quasienergies of states for which the partial waves with $N\leq-10$ all contribute for less than 10% to the norm of the wave function, the norm being calculated as the cycle-average overlap of the wave function with the complex conjugate of its dual [13].

As is shown in Fig. 6, the $5p$ quasienergy curve changes its high intensity limit between 480 and 490 nm through a laser-induced degeneracy with a state with unphysical characteristics. At 480 nm, the $5p$ state follows the trajectory represented by a red solid line in that diagram, which brings it close to the state following the solid black curve. The latter is not indicated in Fig. 5. It cannot be followed much below $\alpha_0=3$ a.u., because of its excessively large ionization width, and it rapidly disappears from the Brillouin zone for $\alpha_0 \gg 3$ a.u. However, it has no unphysical features at $\alpha_0 \approx 3$ a.u., where it interacts with the $5p$ and $7p$ quasienergy curves. It is best seen as an instance of a light-induced state without counterpart in the field-free spectrum [19,28]. At 490 nm, the low-α_0 $5p$ state follows the red dashed curve as α_0 increases and the high-α_0 $7p$ state follows the black dashed curve as α_0 decreases; both therefore evolve into unphysical states.

Large scale changes similar to those discussed in Sec. III A can also be found in Fig. 5, notably between 500 and 550 nm, around $\alpha_0=7$ a.u., where the low-α_0 $6p$ curve reconnects to the high-α_0 $5p$ curve. Also noteworthy is the arrival of a state with an unphysical high-intensity limit at 600 nm, at Re $\epsilon\approx-0.015$ a.u. and $\alpha_0\approx 11$ a.u. The downward progression of this state at longer wavelengths is ac-

companied by a reorganization of the spectrum around $\alpha_0 = 12$ a.u., between 600 and 650 nm, and then the appearance of a quasienergy curve shifting rapidly downward between $\alpha_0 = 12$ and 14 a.u. from 700 nm onward.

The absence above 550 nm of avoided crossings between the dressed low excited states and the dressed ground state is also worth noting. For a fixed α_0, the ionization width of the dressed ground state decreases when the wavelength increases, since its coupling to the continuum requires the absorption of more and more photons. Unless the intensity is too high, its width becomes sufficiently small compared to the width of the dressed low excited states that their crossings are all direct rather than avoided.

That the high-α_0 part of the spectrum varies comparatively little with wavelength is visible from Figs. 4 and 5. In fact, for high values of α_0 the dressed excited states tend to follow the same trajectories in the quasienergy spectrum of argon as in that of atomic hydrogen, at all wavelengths in the visible (Fig. 7).

[In Fig. 7(a), the data points tracing an arc of parabola belong to a deeply bound state dressed by the field.] The agreement between these two species generally improves as α_0 increases, as can be seen by comparing Fig. 7(b) to Fig. 7(a). As noted above, the short range part of the potential becomes of lesser importance when the intensity increases, since the active electron has a higher and higher probability to be far from the nucleus and its dynamics is more and more dominated by its interaction with the field.

To compare with argon, we show, in Fig. 8, how the $(\sigma = -1, m = 0)$ spectrum of lithium, sodium, potassium, and rubidium evolve between 400 and 800 nm. Also given in this figure are the corresponding results for atomic hydrogen. Except at the lowest values of α_0, at 400 nm the four alkali metals are similar to each other and to hydrogen. Between 400 and 800 nm, the spectra of potassium and of rubidium changes in the same way as the spectrum of argon discussed above, while lithium and sodium remain closer to atomic hydrogen. However, in all four cases the high-α_0 quasienergy curves tend to follow the same trajectories as the dressed states of atomic hydrogen. As the wavelength increases, the spectrum at medium values of α_0 evolves from one dominated by dressed excited states shifting little to one dominated both by states shifting rapidly downward and by states shifting rapidly upward. The former are expected at long wavelengths, since states for which $I_p \ll \hbar\omega$ have a Stark shift roughly equal to $-U_p$. The occurrence of the latter is more surprising, although it is known that states for which $I_p \approx \hbar\omega$ tend to have a large positive Stark shift [19] and that the bound states of the dressed Coulomb potential also move rapidly upward for (small) increasing values of α_0 [29].

Finally, we note that the spectrum of hydrogen undergoes a similar reorganization between 600 and 800 nm as that discussed above in relation to Fig. 6. Laser-induced degeneracies with light-induced states are therefore possible even when the potential is purely Coulombic.

IV. CONCLUSIONS

In conclusion, we have shown how representative regions of the quasienergy spectrum of argon and of four alkali metals evolve when the wavelength of the laser field varies from the uv to the near infrared. While their fine details are species-specific, the main features of the spectra of potassium, rubidium, and argon are similar. For all atoms, the quasienergy curves tend to follow the same trajectories at high intensities. How the high-intensity spectrum connects to the field-free spectrum depends on the wavelength. The relation between the two parts of the spectrum is affected by the intrusion of resonant low lying states among the dressed excited states. Large-scale changes in the topology of the spectrum also arise from laser-induced degeneracies with states without physical high-intensity or low-intensity limits.

These general features are likely to be generic and to apply to any atomic species whose dynamics in a strong laser field can be represented by that of a single-active electron. We thus expect that the quasienergy maps presented here can be used as a rough guide to the positions of Freeman resonances arising from nonponderomotively shifted low lying states. The occurrence of light-induced degeneracies would manifest by a rapid change with wavelength in the positions of the corresponding resonance structures in the ATI spectrum, provided the states involved have a sufficiently long ionization lifetime for these structures to be observable.

ACKNOWLEDGMENTS

E.M. thanks COST P14, TÜBİTAK, and DÜAPK for the support provided for this project. Part of the calculations presented have been performed on computers financed by the EPSRC.

[1] J. H. Shirley, Phys. Rev. **138**, B979 (1965).
[2] R. M. Potvliege and R. Shakeshaft, Adv. At., Mol., Opt. Phys. Suppl. **1**, 373 (1992).
[3] C. J. Joachain, M. Dörr, and N. J. Kylstra, Adv. At., Mol., Opt. Phys. **42**, 225 (2000).
[4] H. C. Day, B. Piraux, and R. M. Potvliege, Phys. Rev. A **61**, 031402(R) (2000).
[5] S.-I Chu and D. A. Telnov, Phys. Rep. **390**, 1 (2004).
[6] Y. Gontier and M. Trahin, Phys. Rev. A **7**, 1899 (1973).
[7] R. R. Freeman, P. H. Bucksbaum, H. Milchberg, S. Darack, D. Schumacher, and M. E. Geusic, Phys. Rev. Lett. **59**, 1092 (1987).
[8] H. G. Muller and F. C. Kooiman, Phys. Rev. Lett. **81**, 1207 (1998).
[9] H. G. Muller, Phys. Rev. A **60**, 1341 (1999).
[10] H. G. Muller, Phys. Rev. Lett. **83**, 3158 (1999).
[11] M. J. Nandor, M. A. Walker, L. D. Van Woerkom, and H. G. Muller, Phys. Rev. A **60**, R1771 (1999). See also L. D. Van Woerkom *et al.*, www.physics.ohio-state.edu/~lvw/what/singlee/singlee.html; and L. D. Van Woerkom, M. A. Walker,

M. J. Nandor, and H. G. Muller, in *Multiphoton Processes*, edited by L. F. DiMauro, R. R. Freeman, and K. C. Kulander (American Institute of Physics, Melville, NY, 2000), p. 70.
[12] J. Wassaf, V. Véniard, R. Taïeb, and A. Maquet, Phys. Rev. Lett. **90**, 013003 (2003); Phys. Rev. A **67**, 053405 (2003).
[13] R. M. Potvliege and S. Vučić, Phys. Rev. A **74**, 023412 (2006).
[14] See, e.g., Shih-I Chu and J. Cooper, Phys. Rev. A **32**, 2769 (1985); A. Giusti-Suzor and P. Zoller, Phys. Rev. A **36**, 5178 (1987); R. M. Potvliege and R. Shakeshaft, Phys. Rev. A **40**, 3061 (1989); S.-I Chu, K. Wang, and E. Layton, J. Opt. Soc. Am. B **7**, 425 (1990); M. Crance, J. Opt. Soc. Am. B **7**, 449 (1990); M. S. Pindzola and M. Dörr, Phys. Rev. A **43**, 439 (1991); M. Dörr, R. M. Potvliege, D. Proulx, and R. Shakeshaft, Phys. Rev. A **43**, 3729 (1991); H. Rottke, B. Wolff-Rottke, D. Feldmann, K. H. Welge, M. Dörr, R. M. Potvliege, and R. Shakeshaft, Phys. Rev. A **49**, 4837 (1994); A. Buchleitner, D. Delande, and J.-C. Gay, J. Opt. Soc. Am. B **12**, 505 (1995); M. Plummer and C. J. Noble, J. Phys. B **33**, L807 (2000); A. Buchleitner, D. Delande, and J. Zakrzewski, Phys. Rep. **368**, 409 (2002).
[15] E. Meşe and R. M. Potvliege, Laser Phys. Lett. **4**, 357 (2007).
[16] J. I. Gersten and M. H. Mittleman, J. Phys. B **9**, 2561 (1976).
[17] M. Gavrila and J. Z. Kaminski, Phys. Rev. Lett. **52**, 613 (1984).
[18] M. Gavrila, Adv. At., Mol., Opt. Phys. Suppl. **1**, 435 (1992).
[19] A. S. Fearnside, R. M. Potvliege, and R. Shakeshaft, Phys. Rev. A **51**, 1471 (1995).
[20] C. R. Holt, M. G. Raymer, and W. P. Reinhardt, Phys. Rev. A **27**, 2971 (1983).
[21] R. M. Potvliege and R. Shakeshaft, Phys. Rev. A **40**, 3061 (1989).
[22] M. Pont and R. Shakeshaft, Phys. Rev. A **43**, 3764 (1991).
[23] M. Pont, R. M. Potvliege, R. Shakeshaft, and P. H. G. Smith, Phys. Rev. A **46**, 555 (1992).
[24] O. Latinne, N. J. Kylstra, M. Dörr, J. Purvis, M. Terao-Dunseath, C. J. Joachain, P. G. Burke, and C. J. Noble, Phys. Rev. Lett. **74**, 46 (1995).
[25] A. Cyr, O. Latinne, and P. G. Burke, J. Phys. B **30**, 659 (1997).
[26] M. Klapisch, C. R. Seances Acad. Sci., Ser. B **265**, 914 (1967).
[27] R. M. Potvliege, Comput. Phys. Commun. **114**, 42 (1998). The Fortran code is distributed by the Computer Physics Communications Program Library.
[28] R. M. Potvliege, Phys. Scr. **68**, C18 (2003).
[29] M. Pont, N. R. Walet, and M. Gavrila, Phys. Rev. A **41**, 477 (1990).